

understanding and mapping how the magnitude(s) of this natural frequency(s) changes as degradation itself manifests.

CHAPTER 10: ROADMAP FOR SUMMER

The fundamental project of this work is to pay attention to and identify any change in the response data once damage is introduced – such that it is possible to reliably identify similar emergent damage in future structures. This year's experimental analyses will use the same physical turbine model as the previous student; the same shaker table; the same two accelerometers.

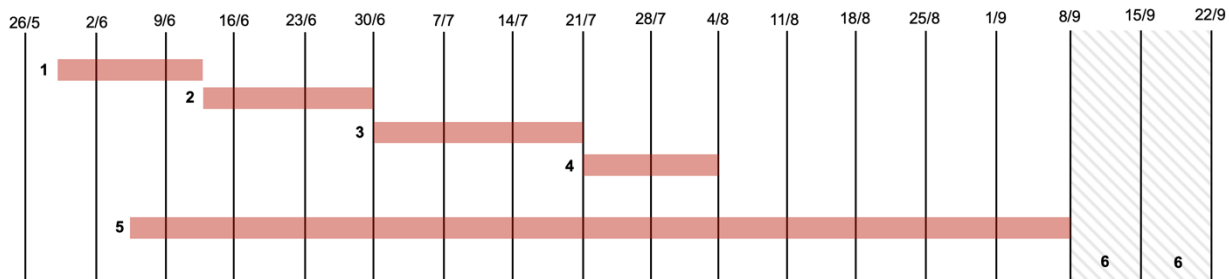
This year's project will still apply sinusoidal forces at discrete frequencies – although it is suspected that it is a mistake to persist with discrete excitation frequencies without coupling this understanding with an ascending continuous sweep. This is because the emergent excitation frequencies found in nature are not inherently discrete or necessarily aligned with those selected for the experiment. The resonant frequencies of the structure are not known to occupy any of the preselected excitation frequencies; they will likely fall between the bands and could contain crucial information about emergent signatures of degradation. As such – discrete only excitation frequencies will give a fragmented understanding of the system's behaviour.

The three core intentions of this year's project are to:

- **Core Intention 1:** Decrease the magnitude of the interval between the excitation frequencies for the same upper and lower limits such that more excitation frequencies are trialed.
- **Core Intention 2:** Attempt to build a Fast Fourier Transform engine in Python.

- **Core Intention 3:** Attempt to communicate more clearly – both in the project work itself and in the final dissertation – the distinct signatures of emergent degradation in the response frequencies and their amplitudes; perhaps via the incorporation of this understanding into a confusion matrix that can be trialed and verified.

The author's attention will initially be focused on bolt removal as damage [Tests 7, 8, 9 in the previous student's work] and will only move to pad addition as damage [Tests 5 and 6] if the former becomes sufficiently mapped. Bungee cords [Test 10] and reorientation of the static rotor [Test 4] will not be assessed. A Gantt chart of this year's summer project is provided below; however this is subject to adjustment based on its natural evolution.



- 1: Collect Data / Experimental Work (Core Intention 1).
- 2: Build an FFT in Python (Core Intention 2).
- 3: Analyse the data and generate a Confusion Matrix (Core Intention 3).
- 4: Test the Confusion Matrix with New Data (Core Intention 3).
- 5: Write the Dissertation Alongside.
- 6: Unavailable due to Existing Commitments.

Figure 46: Gantt Chart of the summer project.

The following ideas are strong questions for further research but probably fall outside of what is realistically possible given the time available to complete the project:

- The addition of a motor to the rotor such that it is possible to map the change in frequency response pre and post damage while the unit is actually operational – given that the real system will have a non-zero rotational velocity of its rotor for approximately 93.5% of the time; that hence this understanding is essential.

- Identify with a high fidelity the natural frequencies of the structure pre and post damage by rerunning tests with very small intervals about their established approximate magnitudes, i.e., “zeroing in” to enable a mapping of the natural frequencies *without* the need for a continuous ascending sweep.

Perhaps these two ideas can be built on in years to come by future students once the three core intentions of this year’s project have been satisfied.

CONCLUSION

The transition to offshore wind power is a critical step in the global response to climate change, but its success depends not just on energy yield, but on the long-term resilience of the infrastructure deployed. This report has outlined the technical and environmental case for offshore wind, with a specific focus on jacket foundation design and the role of condition monitoring in preserving structural integrity over decades of exposure. Through an examination of failure modes, sensing technologies, and recent literature - particularly in vibrational analysis using accelerometers - it becomes clear that the field is shifting from breakdown to predictive maintenance strategies. The most promising advances lie at the intersection of mechanical engineering and artificial intelligence, where machine learning models can be trained to detect the subtle precursors to failure before catastrophic collapse. However, many of these models remain poorly benchmarked against the physical forces acting on real structures; experimental designs often fail to match the complexity of operational systems. The work ahead - including the planned summer project - aims to bridge this gap. By refining excitation strategies, improving frequency resolution, and clarifying the relationship between response profiles and specific forms of degradation, this project seeks to contribute to scalable, trustworthy condition monitoring solutions in the next generation of offshore infrastructure.

REFERENCES:

- Adafruit Industries. *Anemometer Wind Speed Sensor w/Analog Voltage Output*. Available at: <https://www.adafruit.com/product/1733> [Accessed 8 March 2025]
- Ahmad, N., Bihs, H., Kamath, A., Arntsen, Ø. A. Numerical Modelling of Scour around an Offshore Jacket Structure using REEF3D.
- Azad, K., Rasul, M., Halder, P., Sutariya, J. 2019. Assessment of Wind Energy Prospect by Weibull Distribution for Prospective Wind Sites in Australia. *Energy Procedia*. 160, pp. 348-355. doi: 10.1016/j.egypro.2019.02.167.
- Bakhoday-Paskyabi, M., Krutova, M., Bui, H., Ning, X. 2022. Multiscale Simulation of Offshore Wind Variability During Frontal Passage: Brief Implication on Turbines' Wakes and Load. *Journal of Physics: Conference Series*. 2362. doi: 10.1088/1742-6596/2362/1/012003.
- Baquerizo, J., Tutivén, C., Puruncajas, B., Vidal, Y., Sampietro, J. 2022. Siamese Neural Networks for Damage Detection and Diagnosis of Jacket-Type Offshore Wind Turbine Platforms. *Mathematics*. doi: 10.3390/math10071131.
- Bamber, J. L., Griggs, J. A., Hurkmans, R. T. W. L., Dowdeswell, J. A., Gogineni, S. P., Howat, I., Mouginot, J., Paden, J., Palmer, S., Rignot, E., Steinhage, D. 2013. A new bed elevation dataset for Greenland. *The Cryosphere*, 7, pp. 499-510. doi: 10.5194/tc-7-499-2013.
- Bašić, M., Vukadinović, D., Polić, M. 2018. Stray Load and Iron Losses in Small Induction Machines Under Variable Operating Frequency and Flux: A Simple Estimation Method. *IEEE Transactions on Energy Conversion*. 33(2). doi: 10.1109/TEC.2017.2759816.
- Borgelt, J., Possekell, J., Schaumann, P., Dreger, D., Ghafoori, E. 2024. Innovative test concept for evaluating fatigue degradation process of submerged grouted connections. *Engineering Structures*, 302. doi: 10.1016/j.engstruct.2023.117335.
- BUCHER hydraulics. *Wind Turbines*. Available at: <https://www.bucherhydraulics.com/en/areas-of-use/energy/wind-turbines> [Accessed 8 March 2025]
- Chen, T., Wang, X., Gu, X., Zhaoa, Q., Yuan, G., Liu, J. 2019. Axial compression tests of grouted connections in jacket and monopile offshore wind turbine structures. *Engineering Structures*, 196. doi: 10.1016/j.engstruct.2019.109330.
- Christ, A. J., Bierman, P. R., Schaefer, J. M., Dahl-Jensen, D., Steffensen, J. P., Corbett, L. B., Peteet, D. M., Thomas, E. K., Steig, E. J., Rittenour, T. M., Tison, J Blard, P., Perdrial, N., Dethier, D. P., Andrea Lini, A., Hidy, A. J., Caffee, M. W., Southon, J. 2021. A multimillion-year-old record of Greenland vegetation and glacial history preserved in sediment beneath 1.4 km of ice at Camp Century. *PNAS*. 118(13). doi: 10.1073/pnas.2021442118.
- Cock, O. 2024. Testing the Effect of Various Frequencies and Variables on the Structural Integrity of a Lattice/Jacket Offshore Wind Turbine Foundation.
- DAELIM. *The Ultimate FAQ Guide to Wind Transformers*. Available at: <https://www.daelimtransformer.com/wind-transformer.html> [Accessed 8 March 2025]
- Dehtyriov, D., Schnabl, A. M., Vogel, C. R., Draper, S., Adcock, T. A. A., Willden, R. H. J. 2021. Fractal-like actuator disc theory for optimal energy extraction. *J. Fluid Mech.* 927. doi: 10.1017/jfm.2021.766.
- Desmos. *Desmos | Graphing Calculator*. Available at: <https://www.desmos.com/calculator> [Accessed: 24 April 2025].
- Encalada-Dávila, A., Pardo, L., Vidal, Y., Terán, E., Tutivén, C. 2022. Conceptual Design of a Vibration Test System Based on a Wave Generator Channel for Lab-Scale Offshore Wind Turbine Jacket Foundations. *J. Mar. Sci. Eng.*, 10(1247). doi: 10.3390/jmse10091247.
- Euro Caltech. *WE570 Wind Direction Sensor*. Available at: <https://www.eurocaltech.com/product-details/?product=19> [Accessed 8 March 2025]

electrek. *New Jersey's first offshore wind farm hits a milestone – and one county is fighting all of it.*
Available at: <https://electrek.co/2023/07/06/new-jersey-first-offshore-wind-farm-ocean-wind-1/>
[Accessed 8 March 2025]

electrek. *The world's first floating offshore wind farm turns 5 – here's how it's going.*
Available at: <https://electrek.co/2022/12/29/worlds-first-floating-offshore-wind-farm-turns-5/>
[Accessed 8 March 2025]

Esgian Wind Analytics. *Projects.*
Available at: <https://wind-analytics.esgian.com>
[Accessed: 26 February 2025].

Falkner, F. 2016. The Paris Agreement and the new logic of international climate politics. *International Affairs*, 92(5), pp. 1107-1125. doi: 10.1111/1468-2346.12708.

Feijóo, M. d. C., Zambrano, Y., Vidal, Y., Tutivén, C. 2021. Unsupervised Damage Detection for Offshore Jacket Wind Turbine Foundations Based on an Autoencoder Neural Network. *Sensors*. doi.org/10.3390/s21103333.

FloodMap. *Flood Map: Elevation Map, Sea Level Rise Map.*
Available at: <https://www.floodmap.net>
[Accessed: 24 April 2025]

Fretwell, P., Pritchard, H. D., Vaughan, D. G., Bamber, J. L., Barrand, N. E., Bell, R., Bianchi, C. 2013. Bedmap2: improved ice bed, surface and thickness datasets for Antarctica. *The Cryosphere*, 7, 375-393. doi: 10.5194/tc-7-375-2013.

Galeotti, S., DeConto, R., Naish, T., Stocchi, P., Florindo, F., Pagani, M., Barrett, P. et al. Antarctic Ice Sheet variability across the Eocene-Oligocene boundary climate transition. *Science*, 352(6281). doi: 10.1126/science.aab0669.

Gasson E. G. W. and Keisling. B. A. 2020. The Antarctic Ice Sheet A Paleoclimate Modeling Perspective. *Oceanography*, 33(2). doi: 10.5670/oceanog.2020.208.

Global Wind Atlas. *Wind Layers.*
Available at: <https://globalwindatlas.info/en/>
[Accessed: 26 February 2025].

Gruber, K., Regner, P., Wehrle, S., Zeyringer, M., Schmidt, J. 2021. Towards global validation of wind power simulations: A multi-country assessment of wind power simulation from MERRA-2 and ERA-5 reanalyses bias-corrected with the global wind atlas. *Energy*. 238. doi: doi.org/10.1016/j.energy.2021.121520.

Grunewald, N., Martinez-Zarzoso, I. 2015. Did the Kyoto Protocol fail? An evaluation of the effect of the Kyoto Protocol on CO₂ emissions. *Environment and Development Economics*, 21. doi: 10.1017/S1355770X15000091.

Hammad, A., Yu, Z. 2024. A semi-analytical approach for dynamic responses of monopile-supported offshore wind turbines subjected to accidental loads. *Applied Ocean Research*, 153. doi: 10.1016/j.apor.2024.104251.

Hermville,, L., Obergassel, W., Ott,, H. E., Beuermann, C. 2015. UNFCCC before and after Paris – what's necessary for an effective climate regime? *Climate Policy*, 17(2). doi: 10.1080/14693062.2015.1115231.

HILTI. *Supporting the World's Largest Offshore Wind Farm.*
Available at: <https://reports.hilti.group/2022/our-stories/supporting-the-worlds-largest-offshore-wind-farm>
[Accessed 8 March 2025]

iStock. *Wind Turbine Hub Closeup Detail.*
Available at: <https://www.istockphoto.com/photo/wind-turbine-hub-closeup-detail-gm180734984-24982495>
[Accessed 8 March 2025]

Kate Morley. *National Grid: Live.*
Available at: <https://grid.iamkate.com>
[Accessed: 7 March 2025]

Lincke, D and Hinkel, J. 2021. Coastal Migration due to 21st Century Sea-Level Rise. *Earth's Future*, 9. doi: 10.1029/2020EF001965.

Ma, Y., Cao, W., Yang, L. Wang, F., Tolbert, L. M. 2017. Virtual Synchronous Generator Control of Full Converter Wind Turbines With Short-Term Energy Storage. *IEEE Transactions on Industrial Electronics*. 64(11). doi: 10.1109/TIE.2017.2694347.

Maritime Business World. *Siemens Gamesa produces 500th offshore wind turbine*. Available at: <https://www.maritimebusinessworld.com/siemens-gamesa-produces-500th-offshore-wind-turbine-2180h.htm> [Accessed 8 March 2025]

McCoy, A., Musial, W., Hammond, R., Hernando, D. M., Duffy, P., Beiter, P., Pérez, P., Baranowski, R., Reber, G., Spitsen, P. Offshore Wind Market Report: 2024 Edition. *National Renewable Energy Laboratory*. Technical Report ID: NREL/TP-5000-90525.

Mehmanparast, A., Taylor, J., Brennan, F., Tavares, I. 2018. Experimental investigation of mechanical and fracture properties of offshore wind monopile weldments: SLIC interlaboratory test results. *Fatigue Fract Eng Mater Struct*. 41. doi: 10.1111/ffe.12850.

Milella. P. P. Fatigue and Corrosion in Metals. Second Edition. *Springer*. doi: 10.1007/978-3-031-51350-3.

Morlighem, M., Rignot, E., Willis, J. K. 2016. Improving Bed Topography Mapping of Greenland Glaciers Using NASA's Oceans Melting Greenland (OMG) Data. *Oceanography*, 29(4), pp. 62–71. doi: 10.5670/oceanog.2016.99.

National Snow and Ice Data Centre. *Explore Data*.

Available at: <https://nsidc.org/data/explore-data>
[Accessed: 24 April 2025]

Otosaka, I. N., Shepherd, A., Ivins, E. R., Schlegel, N., Amory, C., Broeke, M. R. and Horwath, M. 2023. Mass balance of the Greenland and Antarctic ice sheets from 1992 to 2020. *Earth Syst. Sci. Data*, 15, pp. 1597–1616. doi: 10.5194/essd-15-1597-2023.

Okulov, V. L., Sørensen, J. N. 2010. Maximum efficiency of wind turbine rotors using Joukowsky and Betz approaches. *J. Fluid Mech.* 649, pp. 497–508. doi: 10.1017/S0022112010000509.

Pablo Ouro Barba. 2017. Large Eddy Simulation of Tidal Turbines.

Prieto-Galarza, R., Tutivén, C., Vidal, Y. Detection of crack bar deterioration at offshore wind turbine supports using generative adversarial networks and autoencoders. 2024. *Journal of Physics: Conference Series*. doi: 10.1088/1742-6596/2647/18/182010.

Puruncajas, B., Vidal, Y., Tutivén, C. 2020. Vibration-Response-Only Structural Health Monitoring for Offshore Wind Turbine Jacket Foundations via Convolutional Neural Networks. *Sensors*. doi:10.3390/s20123429.

Real Engineering. *The Problem with Wind Energy*.

Available at: <https://www.youtube.com/watch?v=LklIUVkMPI8g>
[Accessed 8 March 2025]

Schlegl, T., Seeböck, P., Waldstein, S. M., Schmidt-Erfurth, U., Langs, G. 2017. Unsupervised Anomaly Detection with Generative Adversarial Networks to Guide Marker Discovery. *IPMI*. doi: 10.48550/arXiv.1703.05921.

Seo, K., Wilson, C. R., Scambos, T., Kim, B., Waliser, D. E., Tian, B., Kim, B. and Eom, J. 2015. Surface mass balance contributions to acceleration of Antarctic ice mass loss during 2003–2013. *Journal of Geophysical Research: Solid Earth*. doi: 10.1002/2014JB011755.

Serat, Z. 2024. Optimizing renewable energy systems for 100% clean energy target: A comparative study of solar, hydro, pumped hydro, and battery storage technologies. *Journal of Energy Storage*. 104. doi: 10.1016/j.est.2024.114441.

Seven Sensor. *Ultrasonic Anemometer*.

Available at: <https://www.sevensensor.com/ultrasonic-anemometer>
[Accessed 8 March 2025]

SPT Offshore. *Wind Turbine Generator (WTG) foundations*.

Available at: <https://www.sptoffshore.com/wind-turbine-generator-wtg-foundations/>
[Accessed 8 March 2025]

SSE. *Laying the foundations for Net Zero on Dogger Bank wind farm*.

Available at: <https://www.sse.com/news-and-views/2022/07/laying-the-foundations-for-net-zero-on-dogger-bank-wind-farm/>
[Accessed 8 March 2025]

Tech2. *Wind turbines yaw system, Yaw Drive Mechanism*.
Available at: <https://www.youtube.com/watch?v=ecT4HvZnaLE>
[Accessed 8 March 2025]

Valdez-Yepeza, R., Tutivénb, C., Vidal, Y. 2024. Structural health monitoring of jacket-type support structures in offshore wind turbines: A comprehensive dataset for bolt loosening detection through vibrational analysis. *Data in Brief*, 53. doi: 10.1016/j.dib.2024.110222.

Vidal, Y., Aquino, G., Pozo, F., Gutiérrez-Arias, J. E. M. 2020. Structural Health Monitoring for Jacket-Type Offshore Wind Turbines: Experimental Proof of Concept. *Sensors*. doi:10.3390/s20071835.

Wang, Y., Walter, R. K., White, C., Kehrli, M. D., Ruttenberg, B. 2021. Scenarios for offshore wind power production for Central California Call Areas. *Wind Energy*. 25. doi: 10.1002/we.2646.

Whitehouse, R. 1998. Scour at marine structures: a manual for practical applications.

Windpower. *Cooling electronics in a hot nacelle*.
Available at: <https://www.windpowerengineering.com/cooling-electronics-in-a-hot-nacelle/>
[Accessed 8 March 2025]

Windpower. *Making of the modern offshore substation*.
Available at: <https://www.windpowerengineering.com/making-modern-offshore-substation/>
[Accessed 8 March 2025]

Winergy. *Winergy HybridDrive*.
Available at: <https://www.youtube.com/watch?v=MUbVEKJJYoA>
[Accessed 8 March 2025]

Wijngaarden, W. A. and Happer, W. 2020. Dependence of Earth's Thermal Radiation on Five Most Abundant Greenhouse Gases. *arXiv*. doi: 10.48550/arXiv.2006.03098.

Worden, K. and Dulieu-Barton, J. M. 2004. An Overview of Intelligent Fault Detection in Systems and Structures. *Structural Health Monitoring*. 3(1). doi: 10.1177/1475921704041866.

World Bank Group. *Electric power consumption (kWh per capita)*.
Available at: <https://data.worldbank.org/indicator/EG.USE.ELEC.KH.PC?end=2019&start=1960>
[Accessed: 26 February 2025].

Wu, X., Hu, Y., Li, Y., Yang, J., Duan, L., Wang, T., Adcock, T., Jiang, Z., Gao, Z., Lin, Z., Borthwick, A., Liao, S. 2019. Foundations of offshore wind turbines: A review. *Renewable and Sustainable Energy Reviews*. 104, pp. 379-393. doi: 10.1016/j.rser.2019.01.012.

Zhang, Y., Zhang, J., Ma, Z., Liu, F., Xu, H., Gu, C., Qiu, H., Wu, R., Qin, L. 2024. Seismic performance evaluation and numerical analysis of CFDST long columns with local corrosion under eccentric compression. *Ocean Engineering*, 306. doi: 10.1016/j.oceaneng.2024.118006.

APPENDIX:

Tables:

	Greenland		Antarctic	
	V _{lost}	V _{remaining}	V _{lost}	V _{remaining}
Year	m ³	% ₁₉₉₂	m ³	% ₁₉₉₂
1992	7.77 × 10 ⁹	100.000%	-3.0 × 10 ¹⁰	100.000%
1993	2.44 × 10 ¹⁰	100.000%	8.02 × 10 ¹⁰	100.000%
1994	1.06 × 10 ¹¹	99.999%	8.93 × 10 ¹⁰	100.000%
1995	4.51 × 10 ¹⁰	99.994%	9.78 × 10 ¹⁰	99.999%
1996	-7.97 × 10 ⁹	99.992%	6.80 × 10 ¹⁰	99.999%
1997	4.68 × 10 ⁹	99.992%	7.55 × 10 ⁹	99.998%
1998	5.45 × 10 ¹⁰	99.992%	1.30 × 10 ¹⁰	99.998%
1999	7.44 × 10 ¹⁰	99.990%	2.09 × 10 ¹⁰	99.998%
2000	2.95 × 10 ¹⁰	99.987%	2.42 × 10 ¹⁰	99.998%
2001	7.68 × 10 ¹⁰	99.985%	3.15 × 10 ¹⁰	99.998%
2002	1.32 × 10 ¹¹	99.982%	2.64 × 10 ¹⁰	99.998%
2003	1.46 × 10 ¹¹	99.976%	6.36 × 10 ¹⁰	99.997%
2004	1.71 × 10 ¹¹	99.970%	7.45 × 10 ¹⁰	99.997%
2005	1.90 × 10 ¹¹	99.963%	6.01 × 10 ¹⁰	99.997%
2006	2.07 × 10 ¹¹	99.954%	7.56 × 10 ¹⁰	99.996%

	Greenland		Antarctic	
	V _{lost}	V _{remaining}	V _{lost}	V _{remaining}
Year	m ³	% ₁₉₉₂	m ³	% ₁₉₉₂
2007	2.35 × 10 ¹¹	99.946%	1.10 × 10 ¹¹	99.996%
2008	2.37 × 10 ¹¹	99.935%	1.16 × 10 ¹¹	99.995%
2009	2.37 × 10 ¹¹	99.925%	1.07 × 10 ¹¹	99.994%
2010	3.07 × 10 ¹¹	99.915%	1.36 × 10 ¹¹	99.994%
2011	3.25 × 10 ¹¹	99.902%	1.80 × 10 ¹¹	99.993%
2012	3.19 × 10 ¹¹	99.888%	1.54 × 10 ¹¹	99.992%
2013	2.13 × 10 ¹¹	99.874%	1.87 × 10 ¹¹	99.991%
2014	1.74 × 10 ¹¹	99.865%	1.98 × 10 ¹¹	99.990%
2015	2.09 × 10 ¹¹	99.857%	1.42 × 10 ¹¹	99.988%
2016	1.65 × 10 ¹⁰	99.848%	7.55 × 10 ¹⁰	99.987%
2017	8.7 × 10 ¹⁰	99.841%	8.56 × 10 ¹⁰	99.987%
2018	1.15 × 10 ¹¹	99.837%	1.58 × 10 ¹¹	99.986%
2019	4.49 × 10 ¹¹	99.832%	2.21 × 10 ¹¹	99.985%
2020	4.45 × 10 ¹¹	99.813%	1.61 × 10 ¹¹	99.984%
2021	3.93 × 10 ¹¹	99.794%	8.67 × 10 ¹⁰	99.983%

Table 1: data from IMBIE – provided in gigatons; converted into m³ and then as a proportion of the remaining volume with 1992 as a baseline (NSIDC 2025).

Figures:

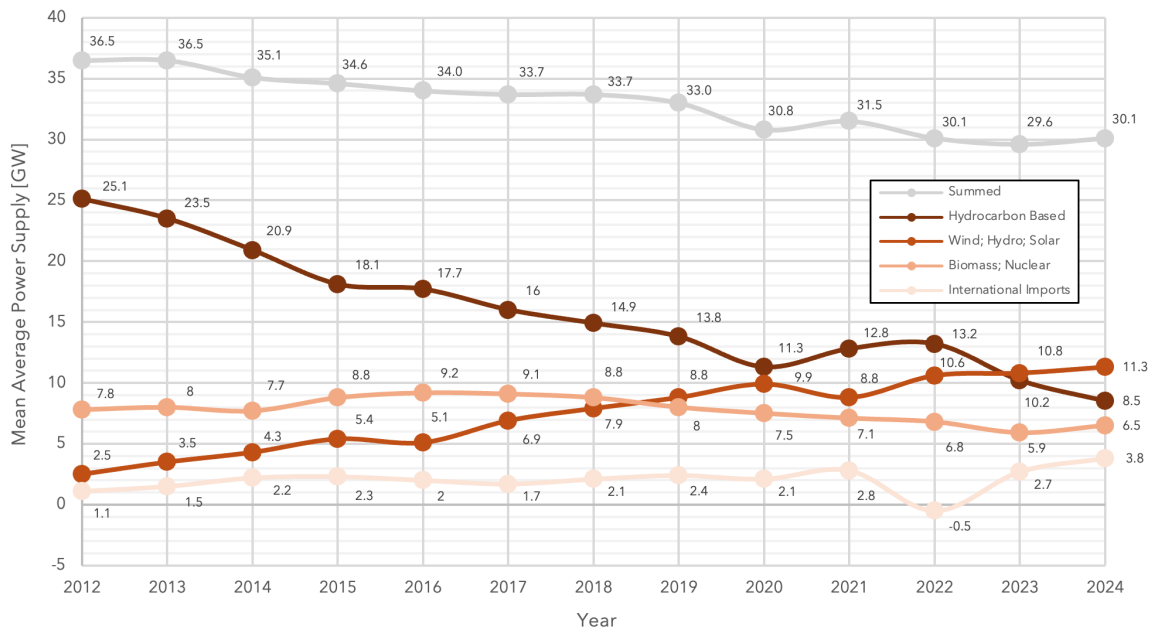


Figure 31: Sources of UK Power from 2012 through 2024 (Morley 2025).

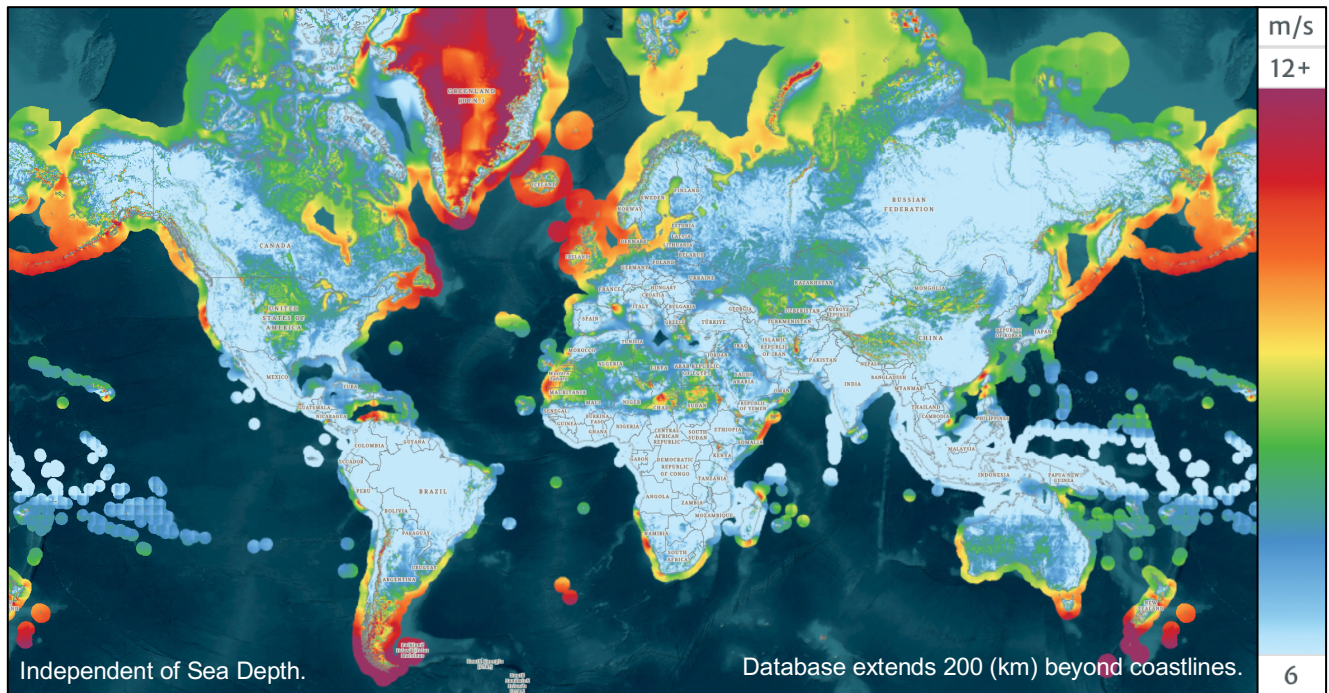


Figure 32: Global Mean Average Wind Speed (Global Wind Atlas 2025).

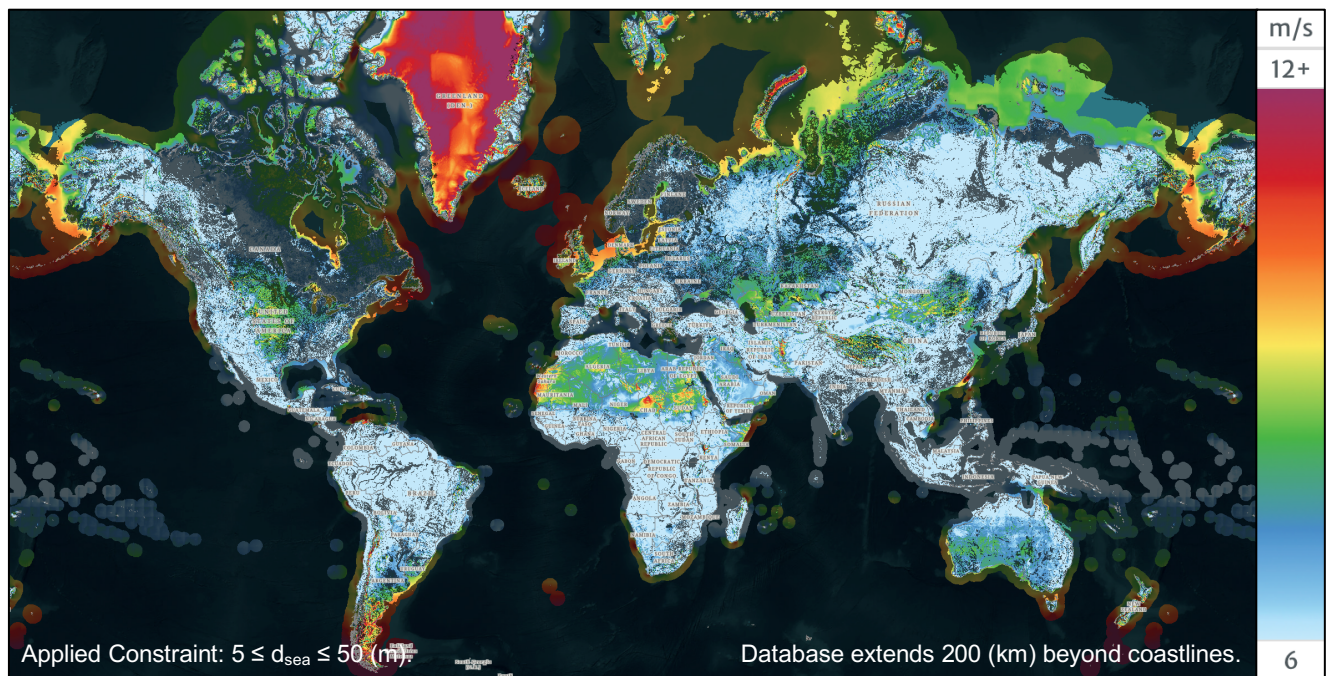


Figure 33: Global Mean Average Wind Speed constrained to sea depths appropriate for Monopile and Jacket foundations (Global Wind Atlas 2025).



Figure 34: Current offshore wind assets in the UK and surrounding regions (Esgian Wind Analytics 2025).

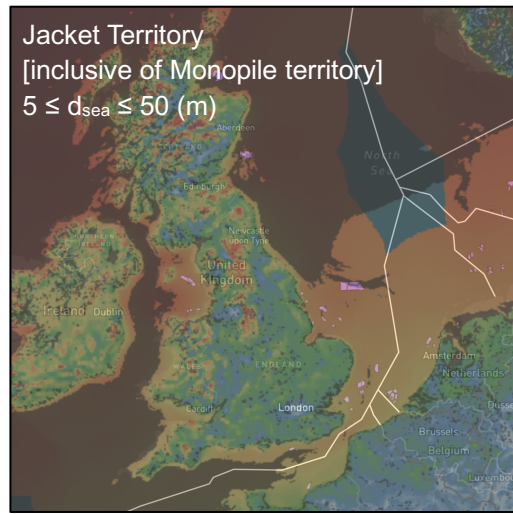


Figure 35: combining asset locations [Figure 4] with Jacket and Monopile appropriate sea depths [Figure 3] (Global Wind Atlas 2025; Esgian Wind Analytics 2025).

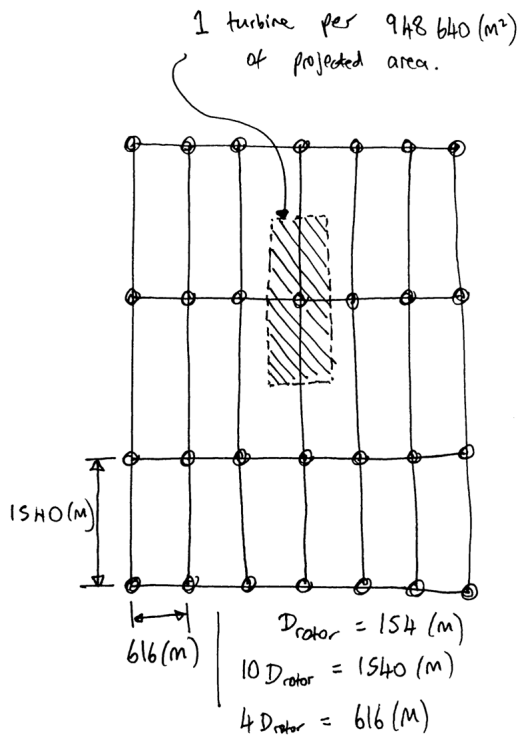


Figure 36: representative array of the SWT-7.0-154.

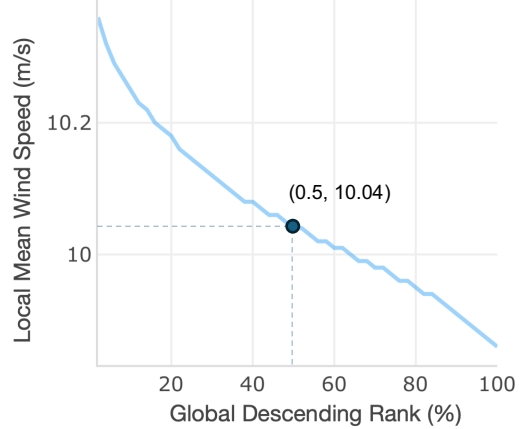
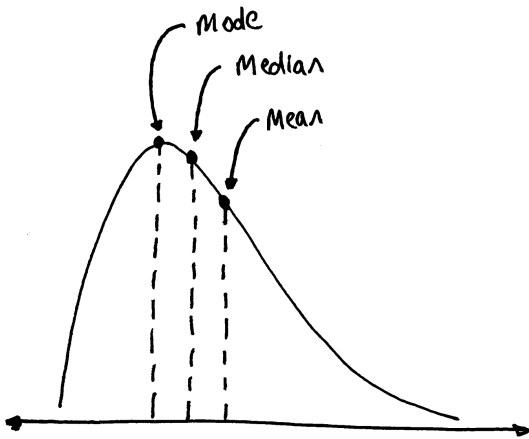


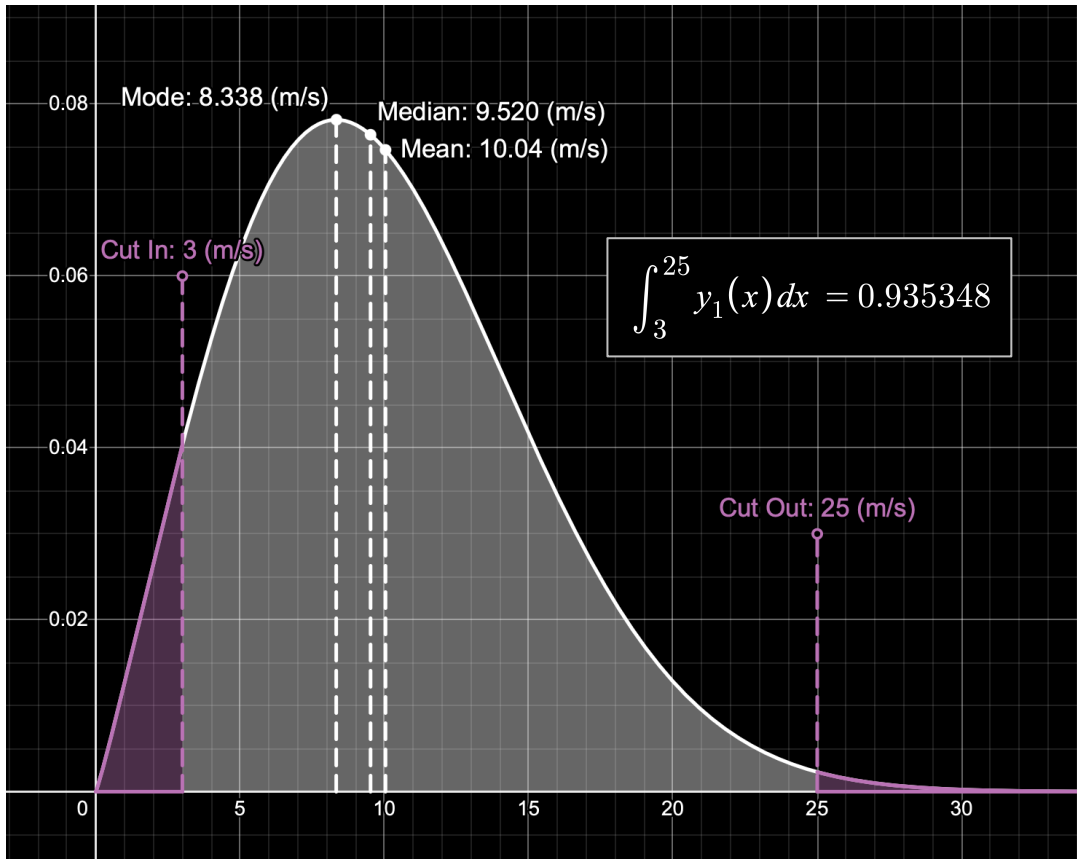
Figure 37: distribution of local mean wind speeds in the sample of Figure 6 (Global Wind Atlas 2025).



Where the Weibull PDF:

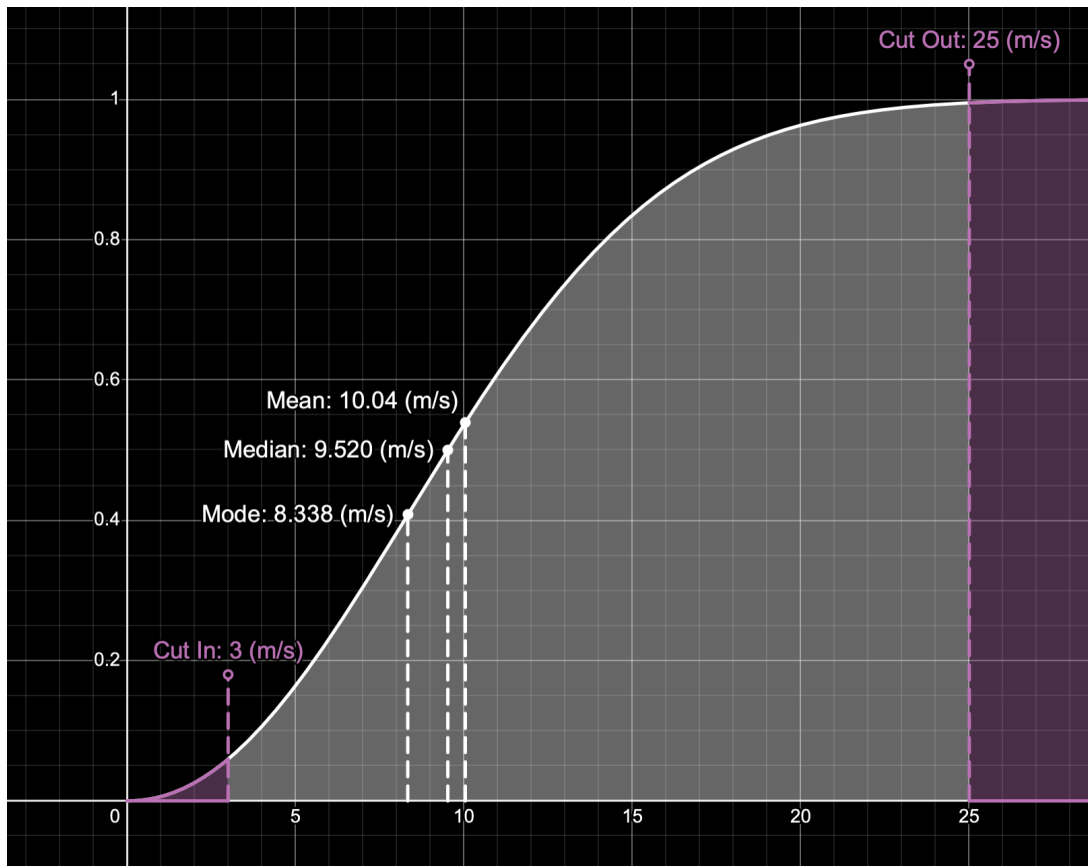
- Skews positively for $0 < k < 3.6$.
- Loosely resembles a Gaussian when $k = 3.6$.
- Skews negatively for $3.6 < k < \infty$.

Figure 38: typical emergent organisation of average types in a positively, i.e. right, skewed Weibull distribution.



$$PDF: \quad y_1(x) = \frac{2.1}{11.3358} \cdot \left(\frac{x}{11.3358}\right)^{(2.1-1)} \cdot e^{-\left(\frac{x}{11.3358}\right)^{2.1}}$$

Figure 39: using the Weibull PDF to model wind speed distribution through time at a fixed location (Desmos 2025).



$$\text{CDF: } y_2(x) = 1 - \left(e^{-\left(\frac{x}{11.3358}\right)^{2.1}} \right)$$

Figure 40: using the Weibull CDF to model wind speed distribution through time at a fixed location (Desmos 2025).



Figure 41: visualising the hydraulic hammer that drives the monopile deep into the sea bed.

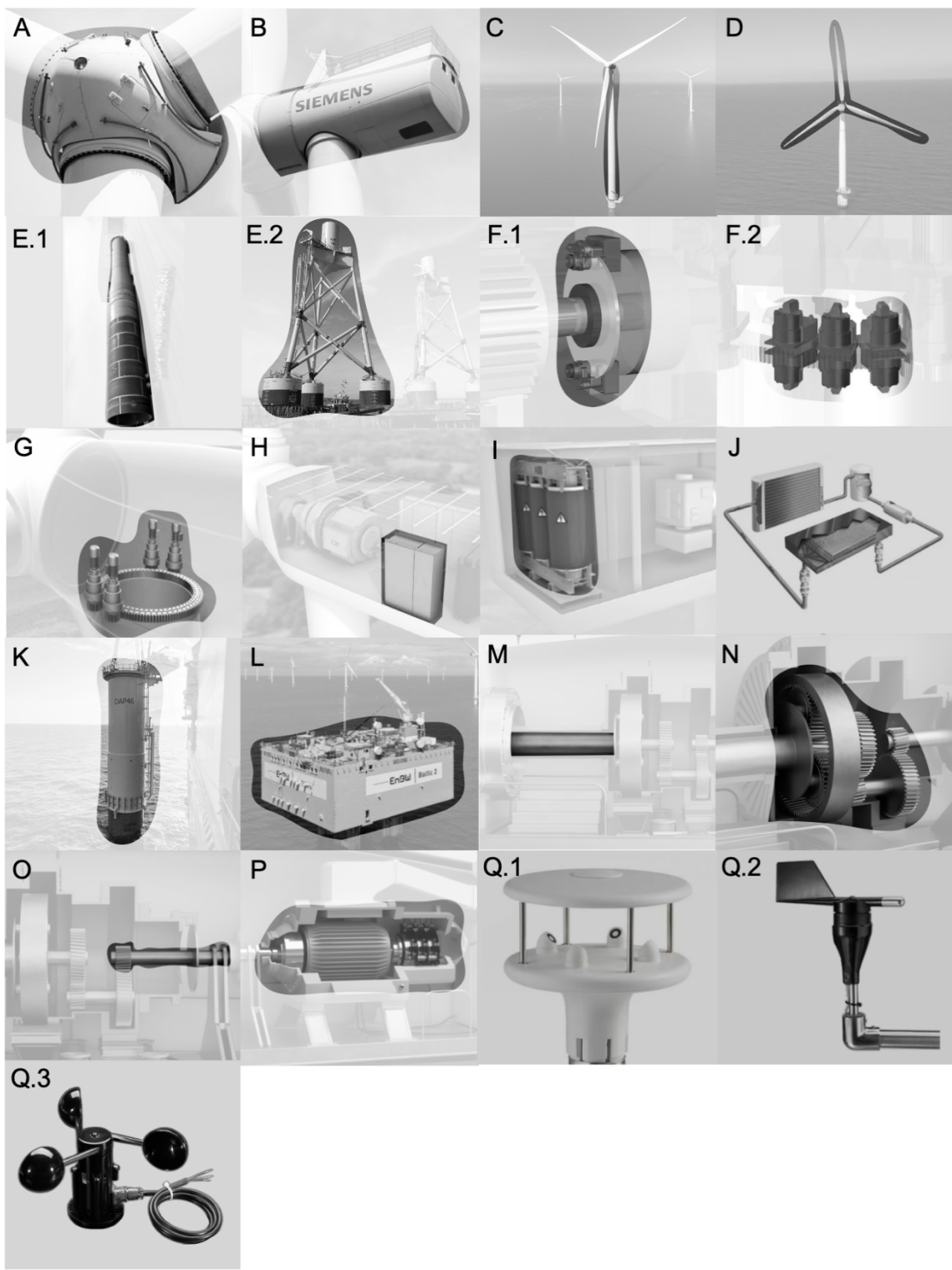


Figure 42: the core components of a modern wind turbine.

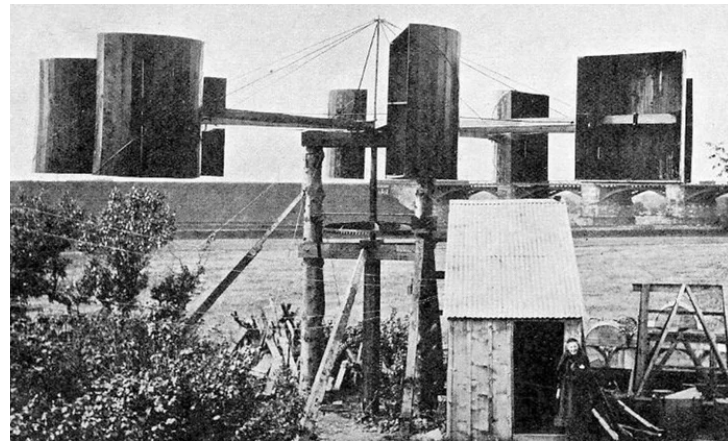


Figure 43: Professor James Blythe's original electrical power generating turbine - circa. 1887; Marykirk, Scotland.

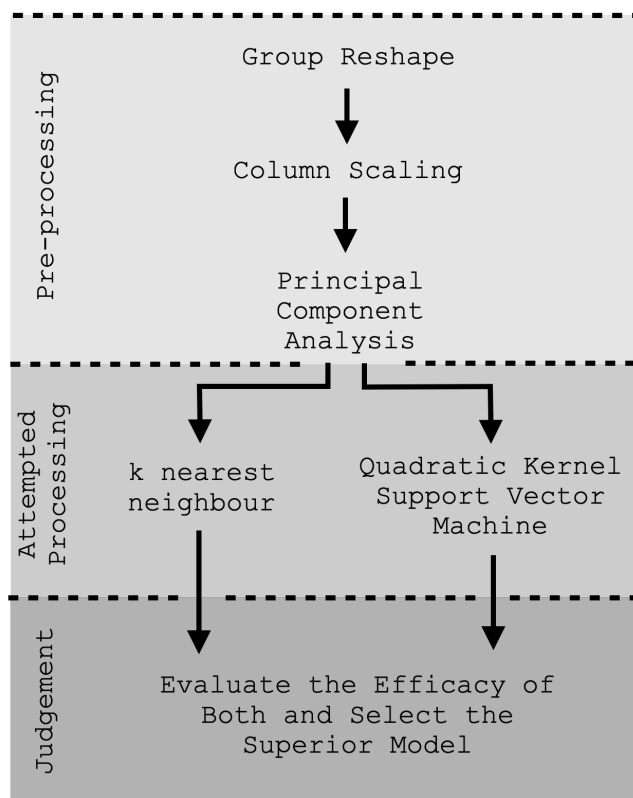


Figure 44: visualising the data processing stages of (Vidal et al 2020).

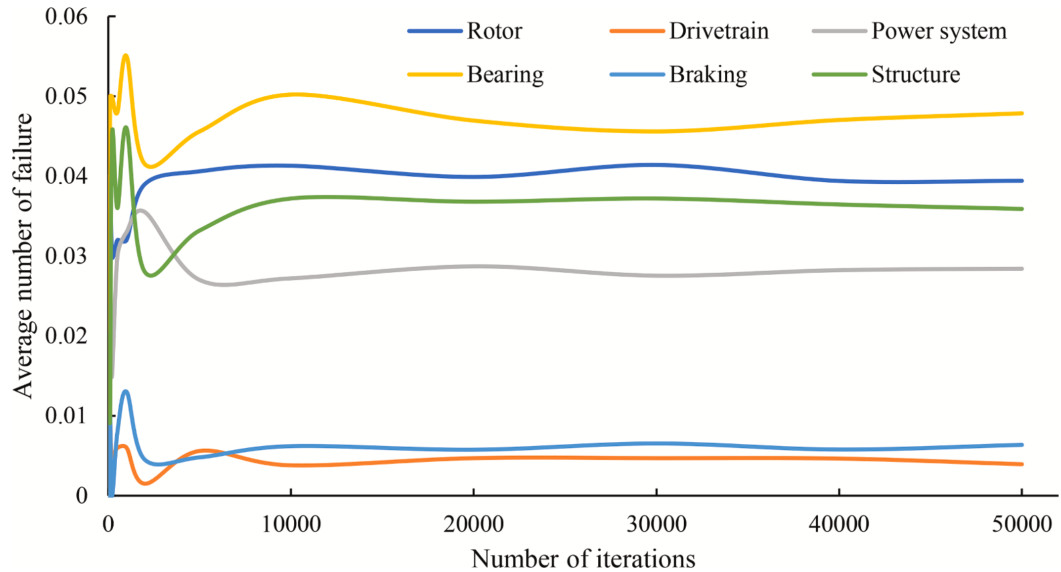


Figure 45: visualising the frequency of emergent degradation amongst the sub-systems in simulation (Yan et al 2023).

Calculations:

$$\text{Calculation 1: } \frac{135\,588\,000\,000}{948\,640} = 142\,929$$

$$\frac{\frac{m^2}{\left(\frac{m^2}{\text{turbine}}\right)}}{\text{turbines}} = \text{turbines}$$

$$\text{Calculation 2: } P_{extractable} = \frac{1}{2} \cdot \rho \cdot A \cdot v^3 \cdot C_P \cdot \eta_M$$

$$(W) = (\text{unity}) \left(\frac{kg}{m^3} \right) (m^2) \left(\frac{m}{s} \right)^3 (\text{unity})(\text{unity})$$

$$= \frac{1}{2} \cdot 1.225 \cdot 5929\pi \cdot (10.04)^3 \cdot 0.45 \cdot 0.95$$

$$= 4,935,994.573$$

$$= \left(\frac{W}{turbine} \right)$$

$$= \mathbf{4.9360} \left(\frac{MW}{turbine} \right)$$

Calculation 3: $(4.9360) (142,929) = 705,497.544$

$$\left(\frac{MW}{turbine} \right) \left(\frac{turbine}{sample} \right) = \left(\frac{MW}{sample} \right)$$

$$= \mathbf{705.5} \left(\frac{GW}{sample} \right)$$

Calculation 4: $\frac{705.50}{33.0} = \mathbf{21.38}$

$$\left(\frac{GW}{GW} \right) = (unity)$$

Calculation 5: $\frac{705.50}{3250.0} = 0.21708$

$$\left(\frac{GW}{GW} \right) = (unity)$$

$$= \mathbf{21.71 \%}$$

Calculation 6: $c = \frac{\nu_{mean}}{\Gamma \left(1 + \frac{1}{k} \right)}$

$$= \frac{10.04}{\Gamma(1.47619)}$$

$$= \frac{10.04}{0.88569}$$

$$= \mathbf{11.3358} \left(\frac{m}{s}\right)$$

Calculation 7: $P_{extractable} = \frac{1}{2} \cdot \rho \cdot A \cdot v^3 \cdot C_P \cdot \eta_M$

$$(W) = (\text{unity}) \left(\frac{kg}{m^3}\right) (m^2) \left(\frac{m}{s}\right)^3 (\text{unity})(\text{unity})$$

$$= \frac{1}{2} \cdot 1.225 \cdot 5929\pi \cdot (9.036)^3 \cdot 0.45 \cdot 0.95$$

$$= \mathbf{3.5983} \left(\frac{MW}{turbine}\right)$$

Calculation 8: $P_{extractable} = \frac{1}{2} \cdot \rho \cdot A \cdot v^3 \cdot C_P \cdot \eta_M$

$$(W) = (\text{unity}) \left(\frac{kg}{m^3}\right) (m^2) \left(\frac{m}{s}\right)^3 (\text{unity})(\text{unity})$$

$$= \frac{1}{2} \cdot 1.225 \cdot 5929\pi \cdot (11.044)^3 \cdot 0.45 \cdot 0.95$$

$$= \mathbf{6.5698} \left(\frac{MW}{turbine}\right)$$
